Biological Psychology 196 (2025) 109024

Contents lists available at ScienceDirect

Biological Psychology

journal homepage: www.elsevier.com/locate/biopsycho

Capturing shared fNIRS responses to visual affective stimuli in young healthy women

Sergio Molina-Rodríguez [a], Carmen Tabernero [b], Joaquín Ibañez-Ballesteros [c,*]

[a] Health Psychology department, Miguel Hernández University, Elche, Alicante, Spain
[b] Instituto de Neurociencias de Castilla y León (INCYL), University of Salamanca, Salamanca, Spain
[c] Department of physiology, Miguel Hernández University, Sant Joan d'Alacant, Sant Joan d'Alacant, Alicante, Spain

ARTICLE INFO

Keywords:
FNIRS
Frequency decomposition
Inter-subject correlation
Affective pictures
Emotional responses

ABSTRACT

Functional near-infrared spectroscopy (fNIRS) studies focusing on prefrontal cortex (PFC) have shown mixed results in relating hemodynamic changes to emotional processing, posing a challenge for clinical practice. Concerns related to instrumentation, recruited sample, task design, signal processing, and data analysis have been highlighted. To minimize some biasing factors, we proposed an experimental approach based on: (1) a homogeneous recruited sample, (2) an identical sequence of content-grouped affective pictures for emotion induction, (3) multi-distance forehead fNIRS recordings to separate cerebral from extra-cerebral components, and (4) a model-free frequency-based analysis to capture shared response patterns across individuals. We piloted a study to assess the feasibility of the approach in a sample of 20 young healthy women during an emotional task with affective pictures of neutral, sexual and violence content. We found coherent fNIRS responses to sexual and violence content located in slow fluctuations (0–0.019 Hz), characterized by positive and negative oxygenation patterns of extra-cerebral and cerebral origin, respectively. Additionally, we corroborated the strong interference of surface hemodynamics. This study proves the feasibility of our approach to identify frequency-specific fNIRS response patterns to affective visual stimuli, which holds promise for exploring functional biomarkers of healthy and altered emotional processing.

1. Introduction

Emotional responses are fundamental to human functioning, but involve multiple cognitive functions that interact across different brain regions (Morawetz et al., 2017), making it challenging to disentangle the underlying neural mechanisms (Saarimäki, 2021). Neuroimaging studies attempt to link emotions and sensor data to find neural biomarkers to objectively assess psychological disorders involving altered emotional processing. As an alternative to model-based approaches, inter-subject correlation (ISC) analysis (Hasson et al., 2004) has been proposed to extract data-driven features from the similarity of neural responses across individuals, without the need to hypothesize the expected response or predefine any model (Adolphs et al., 2016; Nastase et al., 2019).

Through interactions with other brain structures, several subregions of the prefrontal cortex (PFC) have been associated with common and distinct functions in emotion generation and regulation (Dixon et al., 2017; Morawetz et al., 2017). Despite ample empirical evidence for the involvement of the PFC in emotion processing, the precise role and interactions between subregions remains unclear (Doi et al., 2013). Therefore, understanding PFC functions is essential for emotion research and its clinical implications.

For exploring the PFC, simple and friendlier tools using non-intrusive sensors would be useful. Functional near-infrared spectroscopy (fNIRS) is a feasible optical neuroimaging technique that, among other applications (Pinti et al., 2018), shows potential for the study of emotions (Bendall et al., 2016; Doi et al., 2013). fNIRS is comparatively affordable and imposes less discomfort than fMRI (Tuscan et al., 2013) but, in contrast, has limited spatial resolution and cannot reach deep brain regions (Strangman et al., 2013). Fortunately, the most rostral PFC, a subregion involved in emotion processing (Lindquist et al., 2016), can be easily explored by placing the NIRS probe on the hairless skin of the forehead.

A hierarchy of temporal receptive windows has been suggested in which higher order areas, such as the PFC, would require coherent stimulus unfolding over longer time scales (Hasson et al., 2008;

* Correspondence to: Department of physiology, Miguel Hernández University, Santiago Ramon y Cajal Avenue S/N, 03550, Sant Joan d'Alacant, Alicante, Spain.
E-mail address: charly.joa@umh.es (J. Ibañez-Ballesteros).

https://doi.org/10.1016/j.biopsycho.2025.109024
Received 26 August 2024; Received in revised form 12 March 2025; Accepted 2 April 2025
Available online 3 April 2025

Jääskeläinen et al., 2008; Lerner et al., 2011), which implies identifying relevant frequencies to capture consistent ISC, typically bellow 0.1 Hz (Kauppi et al., 2010; Nastase et al., 2019). Since fNIRS provides better temporal resolution than fMRI, it would allow a finer frequency decomposition of hemodynamic responses and a more precise location of their temporal scales. Compared to fMRI and other neuroimaging modalities, less research has been done on ISC using fNIRS. Studies on social interactions by hyperscanning (Nam et al., 2020), music listening (Da Silva Ferreira Barreto et al., 2020) or narratives (Rowland et al., 2018), and movie viewing (Somech et al., 2022) are some notable exceptions.

A stimulus material widely used in neuroimaging studies are scenes from the International Affective Picture System (IAPS) (Bradley & Lang, 2007), which have been shown to be effective in engaging the PFC (Grimm et al., 2009; Morawetz et al., 2017; Northoff et al., 2004). IAPS pictures can be reliably grouped into different blocks of emotional attributes based on their normative values, allowing ISC analysis to be used in a block-design approach providing that the blocks are long enough to obtain reliable correlations (Nastase et al., 2019) and the timing of the stimuli is the same for all individuals (Hejnar et al., 2007; Pajula et al., 2012).

So far, fNIRS studies focusing on PFC have shown mixed results in relating hemodynamic changes to emotional processing. Besides instrumentation issues, differences in recruited sample, experimental paradigms, signal pre-processing and analysis methods have been underlined (Bendall et al., 2016; Westgarth et al., 2021). Problems that could be avoided include sample inhomogeneity, over-removal of low frequencies, inappropriate indicators of task-related hemodynamic activity, and ignoring interference from extracerebral activity (Kirilina et al., 2012; Tachtsidis and Scholkmann, 2016), especially in emotion studies (Simony & Chang, 2020).

Based on this background, we proposed an experimental design combining: (1) a homogeneous recruited sample, (2) a fixed sequence of content-grouped IAPS pictures for emotion induction, (3) multi-distance forehead fNIRS recordings to separate cerebral from extracerebral hemodynamics, and (4) a model-free frequency-based ISC analysis to identify the time-scales of shared response patterns. We hypothesized that, despite large individual variability, participants with similar interpretations of emotional content would have sufficiently similar brain responses to show consistent fNIRS signal time courses, significantly correlated across participants and localized to specific frequency bands. In this pilot study, the proposed approach was tested by conducting a practical experiment under the conditions outlined below.

Given the known influence of gender on emotional experience (Stevens and Hamann, 2012; Whittle et al., 2011) and the greater similarity in women's responses (Finn et al., 2017), we restricted this study to women only. We focus on two types of highly arousing IAPS content: (1) violence, based on the extensive use of negative stimuli in research (Huang et al., 2017) and their particular influence on women's PFC activity (Faraone et al., 2021; Glotzbach et al., 2011; Stevens and Hamann, 2012), and (2) sexual, as additionally to their positive emotional valence may also elicit distinctive autonomic responses. (Bermond et al., 2010; DePesa and Cassisi, 2017; Ritz et al., 2005).

2. Material and methods

2.1. Participants

We recruited twenty-three women from university faculties, all of them right-handed, with normal or corrected-to-normal vision, with no known psychiatric or neurological disorders and self-identified as heterosexual. Only women were selected to avoid gender influences (Stevens & Hamann, 2012) and because their response similarity is usually higher (Finn et al., 2017). As three participants were excluded due to signal quality issues (see 2.5), the final sample was n = 20, with a mean (M) age of 21.25 years and standard deviation (SD) of 2.98 years (range = 18–28 years). This study was approved by the Ethics Committee of university Miguel Hernandez and written informed consent was obtained from all participants.

2.2. Emotional stimuli and procedure

A set of IAPS scenes were used, all depicting interactions between people and with visible faces to enhance emotional response (Groen et al., 2013). Three categories of emotional content were selected based on normative valence and arousal, and adapted to our country's population (Moltó et al., 2013), namely: neutral, sexual (nude hetero couples) and violence (Table 1). Sexual and violence pictures had similar high arousal, but positive and negative valence, respectively. Neutral pictures had medium valence and low arousal.

The experiment took place in the morning, at 10 or 11 am, with the participants sitting comfortably in a softly lit room and with the presence of a single experimenter (a young male psychologist) for all participants. The recording began with a 180-second baseline with participants relaxed while viewing a blank screen. Immediately following the baseline, five blocks of pictures were presented in a fixed order, neutral, sexual, neutral, violence, and neutral. Participants were asked to qualitatively label each picture by simply using two buttons on a response pad, the right for pleasant, the left for unpleasant and neither for neutral/indifferent. Thus, they were not limited to passive viewing but engaged in basic emotional judgement, which also warranted attention. The recording ended with a 180-s recovery period in a relaxed state. Every block contained 13 pictures, each displayed for 5-s followed by a black screen for 1-s to reduce visual persistence. Thus, each block lasted (5 + 1) * 13 = 78-s, within which the pictures were presented in exactly the same order to all the participants (Fig. 1). After recording, participants rated the pictures on a nine-point scale of the Self-Assessment Manikin (SAM) (Bradley & Lang, 1994). Ratings were analysed by repeated measures ANOVA for arousal and valence with the factor "picture category". Post-hoc contrasts were computed for differences.

2.3. fNIRS instrumentation and signal quality check

We used a newly developed NIRS device (Tehia, Newmanbrain, S.L., Elche, Spain) providing 16 short-channels (14 mm) and 12 long-channels (32 mm) (Fig. 2), which was fully described in a previous study by our team (Molina-Rodríguez et al., 2022). The NIRS probe was placed on the forehead, centered on AFpz according to the international 10–5 system (Fig. 2) and overlapping mainly the rostromedial PFC (RMPFC), a subregion commonly targeted in emotion studies (Dixon et al., 2017).

We checked the raw optical data to identify values outside the device's dynamic range or excessive coefficient of variation (> 7.5 %) (Orihuela-Espina et al., 2010; Zimeo Morais et al., 2017) to rule out poor quality recordings. By identifying abrupt changes aligned with accelerometer jumps, we also rejected recordings degraded by motion artifacts. Three participants were excluded after checking, leaving a final

Table 1
Normative arousal and valence of selected pictures.

Selected images	Valence Mean (SD)	Arousal Mean (SD)
Neutral (2036, 2102, 2191, 2235,2384, 2393, 2396, 2397, 2411, 2579, 2593, 2850, 7550)	5.55 (0.51)	3.51 (0.47)
Sexual (4290,4647, 4649, 4652, 4658, 4664.1, 4670, 4672, 4680,4681,4690, 4800, 4810)	6.80 (0.55)	6.73 (0.55)
Violence (3500, 3530, 6212, 6312, 6315, 6520, 6560, 6571, 6834, 9252, 9413, 9414, 9427)	2.07 (0.59)	7.01(0.48)

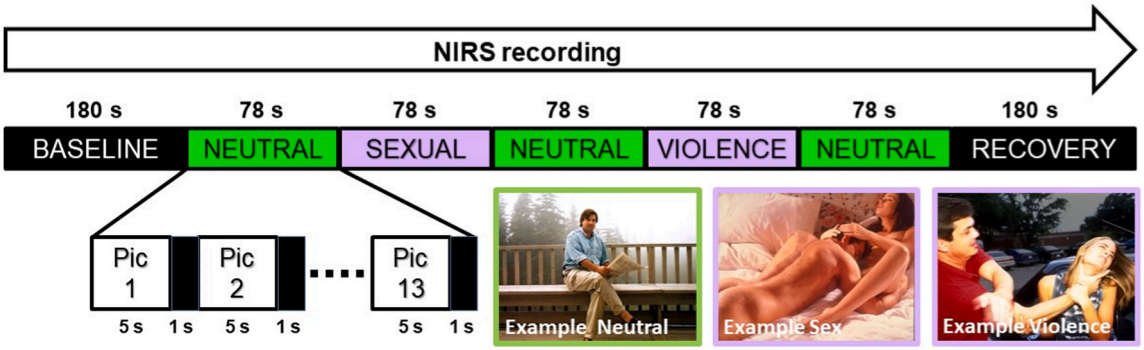

Fig. 1. Schematic diagram of the experimental procedure and examples of pictures per category.

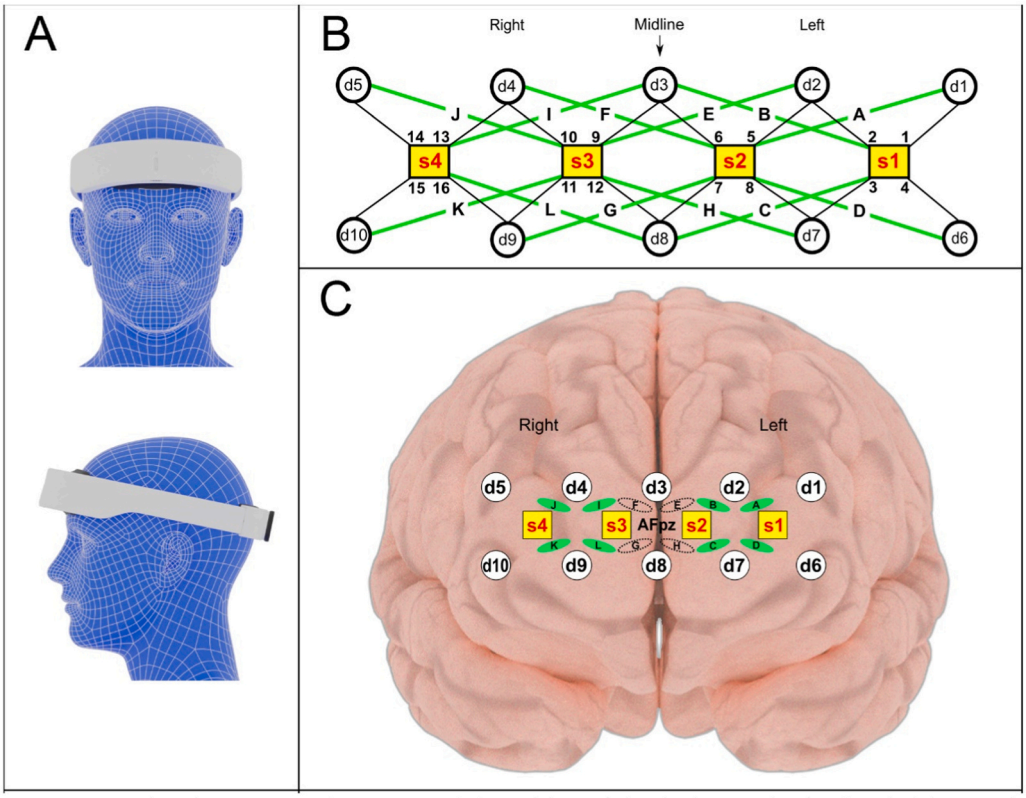

Fig. 2. Probe placement and geometry. (A) Position of the device on the forehead. (B) Optode arrangement (yellow squares = sources; white circles = detectors), providing 16 short-channels (black lines with numbers) and 12 long-channels (green lines with letters). (C) Schematic illustration of the probe over the brain. Green ellipses roughly depict the regions explored by the long-channels. The uncolored ellipses indicate the discarded midline long-channels.

sample of n = 20.

2.4. Signal segmentation and data preprocessing

From the optical raw data, we delimited the 390-s task interval comprised by the five picture blocks (78-s each one). To minimize boundary effects (Cohen et al., 1993) of further processing methods (e.g. wavelet decomposition), we included 30-s of baseline and recovery data to bound a final 450-s data segment (Fig. 3). Thus, for each wavelength, 16 raw data segments were obtained from the short-channels and 12 raw data segments from the long-channels. All post-processing was performed using these data segments and computations were done with MATLAB (Version R2021b, Mathworks, Natick, MA, USA), using native functions, self-made scripts and open-source packages.

Using functions from the Homer2 NIRS package (Huppert et al., 2009), we obtained the relative changes in oxy- (HbO) and deoxy-hemoglobin (HbR) concentration for each channel (Delpy et al., 1988; Kocsis et al., 2006), applying a differential path length calculated as in (Scholkmann & Wolf, 2013). HbO and HbR data were digitally low-pass filtered at 0.2 Hz by a zero-phase 5th-order Butterworth filter to remove respiratory, cardiac and high frequency instrumental components (Huppert et al., 2009). Thus, for each chromophore, we obtained 16 time-series from short-channels plus 12 from long-channels that we called short- (SS) and long-signals (LS), respectively.

2.5. Cerebral signal extraction

Deep fNIRS signals are contaminated by hemodynamic activity not originating in the cerebral cortex (Kirilina et al., 2012; Saager et al., 2011; Takahashi et al., 2011). An effective solution is to use multiple

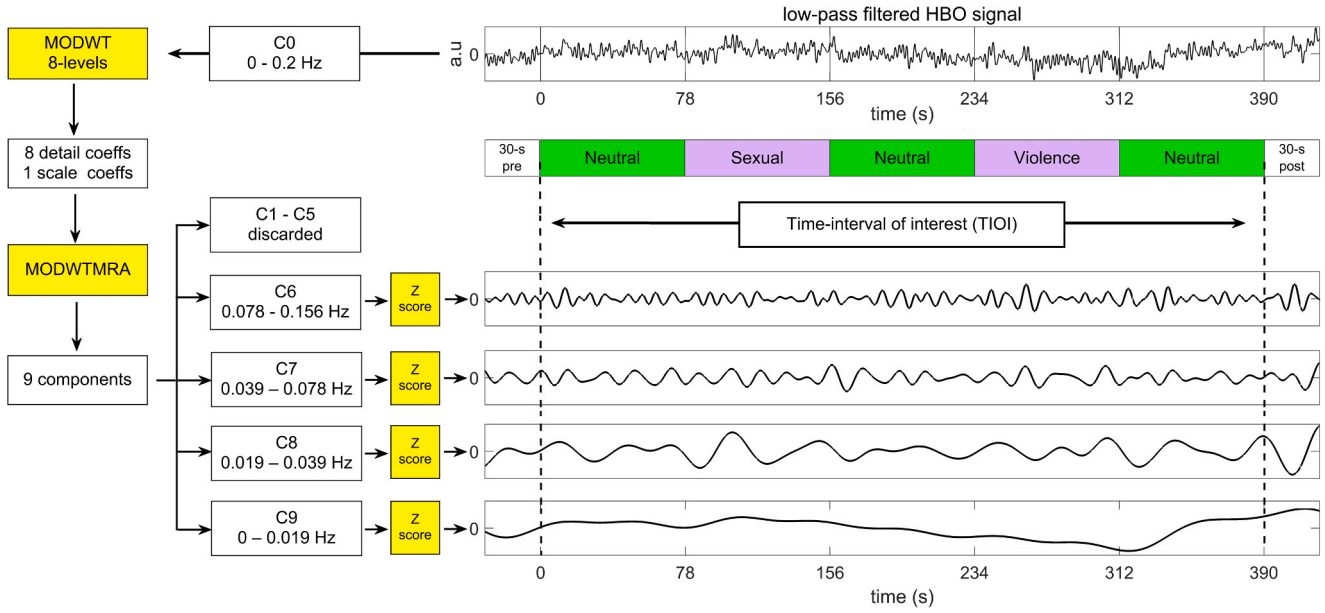

Fig. 3. Schematic diagram of the frequency decomposition procedure.

distance measurements (Pfeifer et al., 2018; Yücel et al., 2017) under the assumption that short-channels only record extracerebral components, whereas long-channels record both extracerebral and cerebral (Brigadoi and Cooper, 2015; Saager and Berger, 2005). Thus, we can use SS data as reference signals to remove surface interference from LS (Gagnon et al., 2011; Scarpa et al., 2013; Zhang et al., 2015).

Among other methods, regression can be applied assuming that physiological noise has correlated time courses in both SS and LS, while the brain task-evoked response is independent (Maruoka et al., 2007; Saager and Berger, 2008; Zhang et al., 2015). Previous studies have shown that surface hemodynamics is spatially inhomogeneous (Gagnon et al., 2011; Kirilina et al., 2012), suggesting that RS be recorded as close as possible to the LS to be decontaminated (Brigadoi and Cooper, 2015; Gagnon et al., 2012). Since the NIRS device provided up to three SS candidates that met the proximity requirements for each LS, we used a "double SS" regressor by combining two SSs into a single reference signal (RS), as suggested in (Gagnon et al., 2014) and following the procedure that was fully described in a previous work by our group (Molina-Rodríguez et al., 2022). In this way, we obtain 12 RSs that will be used as reference signals for the regression of each of the 12 LSs. After regression, we obtained, for HbO and HbR, 12 denoised signals that we denoted as a clean (or corrected) signal (CS) that likely contains the actual cerebral signal.

In this work, we focused on the RS, LS and CS data related to the two regions-of-interest bounded by the four long-channels on the left (A, B, C, D) and the four on the right (I, J, K, L) (Fig. 2, green ellipses). We discarded the midline long-channels (E, F, G, H), avoiding signals measured through the frontal sinus (Haeussinger et al., 2011; Kurihara et al., 2012).

To determine the efficiency in CS extraction, we calculated Pearson correlation coefficients before (RS vs LS) and after regression (RS vs CS) (Erdoğan et al., 2014). The coefficients where "gaussianized" via Fisher's transformation (Silver & Dunlap, 1987) and differences were tested using a two-tailed paired *t*-test. Significance thresholds were adjusted by controlling false discovery rate (FDR) at q= 0.05 (Benjamini and Hochberg, 1995; Singh and Dan, 2006). The data were then back-transformed into r-statistic for reporting.

2.6. Multiband frequency decomposition

Physiological signals are typically nonstationary and, hence, their frequency content can change over time. Wavelet transforms are especially sensitives to nonstationary features and useful for detecting hidden patterns. We employed the undecimated maximal overlap discrete transform (MODWT) (Percival and Walden, 2000; Rhif et al., 2019), which is well suited for synchronization analysis (Bolt et al., 2018; Kauppi et al., 2010) and quite popular for frequency decomposition in neuroimaging research (Kajimura et al., 2023). We implemented an 8-level decomposition using MATLAB's "modwt" function, a Fourier-based implementation of the MODWT, with a Daubechies (db5) wavelet (Daubechies, 1992; Mallat, 2008). After that, we obtained eight sets of detail coefficients plus a final-level of scaling coefficients (Fig. 3). We then applied the function "modwtmra" to compute the multiresolution analysis of the MODWT and obtain nine time-domain oscillatory components, here labelled as C1 to C9, which together perfectly reconstruct the signal. Since "modwtmra" behaves like a zero-phase filter, the components' features exactly line-up with the original signal because they are on the same time scale.

As the upper frequency of the original signals was limited to 0.2 Hz, we only focused on components C6 (0.078–0.156 Hz), C7 (0.039 – 0.078 Hz), C8 (0.019 – 0.039 Hz) and C9 (0 – 0.019 Hz). For consistency, the original signal is referred to here as "C0" and represents the typical preprocessed signal used in most fNIRS studies. Finally, to allow comparisons and averaging procedures the components were standardized into z-scores when necessary (Fig. 3).

2.7. ISC analysis

Since fNIRS uses hemodynamic signals as proxies for neuronal activity (Arne, 2013; Steinbrink et al., 2006), shared fluctuations across participants would be reflected in their synchronized time courses, which can be easily assessed by correlation (Nastase et al., 2019). In this work, we focused on HbO because it meets both a higher sensitivity to forehead surface hemodynamics and a good correlation with fMRI BOLD in the middle frontal area across different cognitive tasks (Cui et al., 2011; Sato et al., 2013). By adopting a *pairwise approach* (Nastase et al., 2019), we computed the symmetric matrix of Pearson's correlation coefficients between the HbO for all combinations of participants' pairs, within each of the five task blocks, and for each channel, component (C0, C6-C9) and signal type (RS, LS, CS). As ISC estimator we calculated the median of the matrix's upper-triangle values, a centrality measure that avoids Fisher transformations and is suitable for parametric and

nonparametric testing (Chen et al., 2016). As sample size was 20, the median was obtained from $(20^2 - 20)/2 = 190$ values, which is enough for ISC analysis (Pajula & Tohka, 2016).

To assess statistical significance, we performed a nonparametric one-sample test through a subject-wise bootstrapping procedure (Chen et al., 2016), under the null hypothesis that the actual data comes randomly from an independent but identical population distribution. For each iteration, the median ISC is calculated after replacing the columns and rows of the correlation matrix with those of N randomly sampled participants with replacement, and then shifted by subtracting the observed ISC (Nastase et al., 2019). We computed the approximated null distributions, over 10.000 resamples, to estimate a *p*-value. The obtained *p*-values were FDR corrected at q= 0.05 (5 task blocks x 8 channels = 40 comparisons). Additionally, we calculated the 95 % confidence interval (CI) by bootstrapping the upper-triangle values of the observed correlation matrix (resamples = 2000).

Merely reaching ISC significance in certain oscillatory component may be misinterpreted, as could occur due to spurious correlations (more likely at lower frequencies). It is necessary to check whether the ISC is also significantly higher than in the others components. We used the test described in (Kauppi et al., 2010; Kauppi et al., 2014), a modified Pearson-Filon statistic based on Fisher's z-transform (ZPF) (Raghunathan et al., 1996), recommended to test for differences between two non-overlapping dependent correlations (Krishnamoorthy & Xia, 2007). Briefly, for each pair of components (a, b) to be compared a ZPF statistics was obtained for all participants pairs in each channel. Then, a sum ZPF statistic ($ZPF^{ab}_{\sum}$) was calculated over all participants pairs. An approximate permutation distribution of $ZPF^{ab}_{\sum}$ was generated by randomly flipping the sign of ZPFs, under the null hypothesis that they come from a distribution with zero mean. Maximal and minimal statistics over all channels were computed for each permutation to finally obtain a symmetric distribution. We generated the null distribution over 20.000 permutations and obtained critical thresholds at $\alpha = 0.05$ against the largest values of the distribution, which implicitly controls the family wise error rate (FWER) for multiple comparisons (Nichols & Holmes, 2002).

Finally, to model the response patterns, we computed the average time-course of HbO and HbR, by channel, component and signal type. Note that, though ISC was not calculated for HbR, it is recommended to contrast both chromophores to better assess fNIRS responses (Tachtsidis & Scholkmann, 2016).

3. Results

3.1. Intra-record judgments and posterior SAM ratings

Pooling the data across all participants, violence pictures were judged as unpleasant in 97 % of the cases. Sexual pictures were rather inconsistent, 43 % pleasant, 24 % unpleasant and 33 % indifferent. Neutral ones were 72 % indifferent and 28 % pleasant.

Regarding SAM ratings, ANOVA test revealed significant effects for valence (F (2, 38) = 62.24, $p < 0.001$, η^2_p= 0.77) and arousal (F (2, 38) = 66.99, $p < 0.001$, η^2_p= 0.76). Post-hoc analysis showed higher valence ratings for sexual (M=7.40, SD=1.46) than for violence (M=2.30, SD=0.69), with no differences for arousal (M=7.77, SD=1.49 and M=8.40, SD=0.73, respectively). Neutral pictures were significantly different for both valence (M=5.17, SD=1.75) and arousal (M=3.95, SD=1.66). These results were consistent with normative values, confirming that participants' emotional states were induced as expected.

3.2. Regression performance

Fig. 4 visualizes a summary statistic of r-values before and after regression. LS was strongly correlated with RS on all channels and components, reflecting a marked contamination of surface hemodynamics. The regression procedure provided a reasonably clean CS, evidenced by the large reduction in correlation. All contrasts (two-tailed paired *t*-test) yielded significant differences ($p < 0.05$, FDR-corrected).

3.3. ISC in CS

No significant ISC was found in any channel or block in components C6 to C8 nor in the original C0 signal (data not shown). However, violence pictures induced strong ISCs in C9 of channels A, C, J and L, reaching significance ($p < 0.05$, FDR corrected) with median values in the range 0.43–0.7 (Fig. 5-CS). The ZPF test confirmed that ISC values were significantly higher in these channels for C9 than for any other component ($p < 0.05$, FWER corrected). Noteworthy, ZPF test was also significant for all other channels. Fig. 5-CS shows the average time courses of HbO and HbR, where a pattern of initial HbO decrease and HbR increase followed by a change in the opposite direction can be observed. This U-shaped HbO pattern explains the strong ISCs found in this block, which are also illustrated as coloured ISC maps in Fig. 6-CS.

3.4. ISC in RS

Again, no significant ISC was found in components C6 to C8 and C0

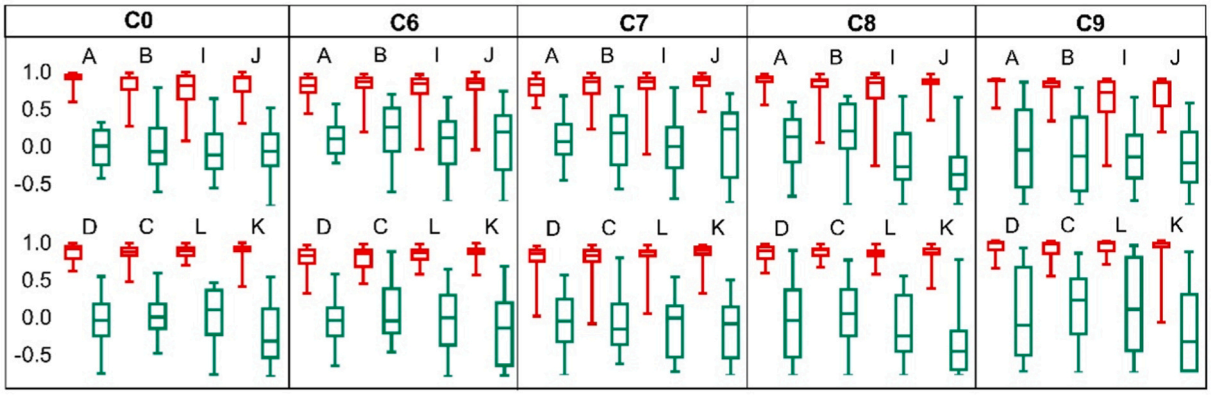

Fig. 4. Regression performance boxplots by component (C0 and C6-C9) and channel. Red and green boxplots correspond to the r-values distribution of LS-RS and CS-RS, respectively. The horizontal line within each box is the sample median while its bottom and top are the 25th and 75th percentiles, respectively. The whiskers lines extend above and below each box to the lowest/largest value within 1.5 times the interquartile range. Channels are labelled with letters. Vertical scales depict the r-values.

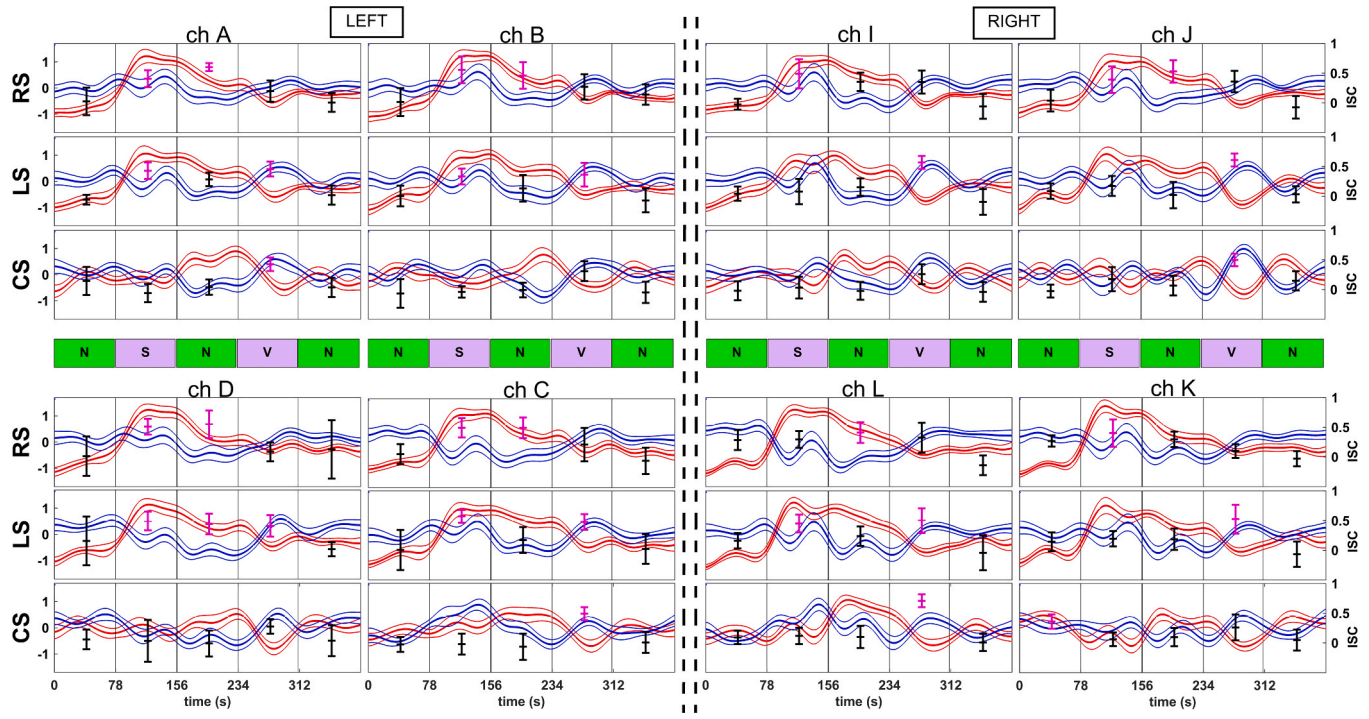

Fig. 5. Average time courses of the z-scored HbO (red) and HbR (blue) in C9. Thick and thin curves depict the mean and the standard error of mean, respectively. The upper three rows correspond to RS, LS and CS for channels A, B, I and J (left to right columns) and the bottom three rows for channels D, C, L and K. Thin vertical lines mark the onset of each picture block, in correspondence with the coloured rectangles drawn in the middle of the graph (N = neutral; S = sexual; V = violence). Within each block, the median ISC and CI (95 %) for HbO are plotted in black (no significant) or magenta (significant; $p < 0.05$, FDR-corrected). HbR time courses are plotted for comparison purposes.

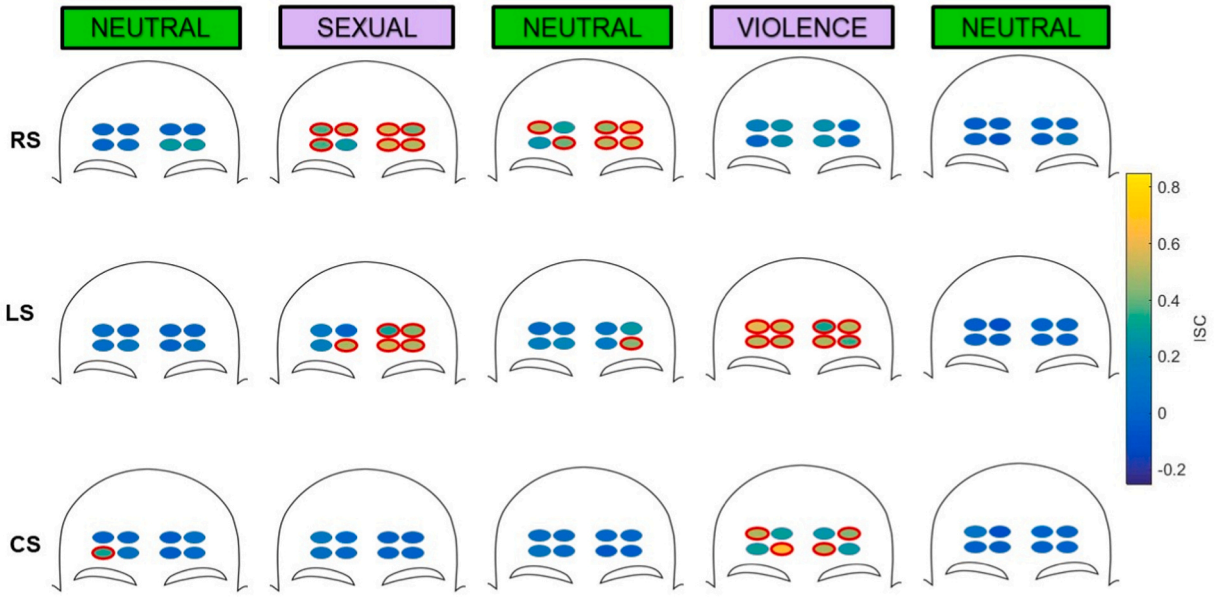

Fig. 6. Illustrative mapping of ISCs onto forehead for all type signals and conditions in C9. Circle colours depict the median ISC. Regions showing significant ISCs are contoured in red.

was also not significant (data not shown). However, sexual pictures triggered consistent responses in C9, even extending to the subsequent neutral block (Figs. 5-RS and 6-RS). This effect was present in all channels except L, with median ISC values ranging from 0.39 to 0.56, and in the form of a common pattern of a sharp increase in HbO along with an initial drop in HbR followed by an increase. The ZPF test showed that ISC values were also significantly higher for all channels in C9 ($p < 0.05$, FWER corrected). Interestingly, violence pictures did not drive coherent responses in RS.

3.5. ISC in LS

Only in C9 were significant ISCs found in five channels for the sexual block (0.33–0.57) and in all the channels for the violence block

(0.36–0.6) (Figs. 5-LS and 6-LS). The time courses look like a combination of RS and CS, suggesting a mixture of shallow and deep components.

4. Discussion

The present work aimed to investigate whether the presentation of a well-structured sequence of affective pictures would induce emotional states long enough to allow the detection of shared responses from multi-distance fNIRS recordings in the forehead. We applied a frequency decomposition of the signals into narrowband oscillatory components, which were in turn subjected to ISC analysis. Notwithstanding the expectable physiological variability between participants and idiosyncratic noise, we found coherent HbO patterns in a sample of young healthy women, which were confined to the lowest frequency band (0 – 0.019 Hz) and were specifically triggered in shallow signals by sexual content and in deep signals by violence. Overall, our findings support the view that negative stimuli would more consistently synchronize PFC activity across individuals, likely recruiting common cerebral circuits relevant to survival, whereas positive stimuli would elicit rather idiosyncratic responses (Nummenmaa et al., 2012). Specifically, they also support that women show a strong engagement of the medial PFC with anger and fear stimuli (Li et al., 2020; Stevens and Hamann, 2012; Whittle et al., 2011), whereas sexual content does not significantly recruit it (Cyders et al., 2016), but triggers changes in surface hemodynamics. They further highlight the importance of controlling surface activity and identifying shared responses on the most informative time scales, in both shallow and denoised deep signals. Before continuing, we would like to point out that our results may be strongly related to the particular IAPS sequence used in this work and may not be generalizable to other picture combinations. The following discussion is not intended to address the underlying emotional mechanisms, but to contrast our results with those of similar studies.

4.1. Superficial and deep separation

LS was strongly correlated with RS in all channels and components (Fig. 4), which corroborates that surface activity is a major source of interference (Kirilina et al., 2012; Tachtsidis and Scholkmann, 2016; Yamada et al., 2012). However, the correlation was greatly reduced for the CS components extracted by multi-distance regression. In C9, violence pictures induced consistent ISCs in both LS (all channels) and CS (four channels), but not in RS, suggesting a deep origin of HbO changes (Fig. 5). It is likely that regression over-attenuated the responses of some individuals and resulted in fewer significant CS channels, which would be supported by the ZPF test.

In contrast, sexual scenes promoted significant ISCs in virtually all RS and LS channels, but none in CS, pointing to a surface origin. Although unlikely, it would not be fully excluded that concurrent, highly correlated, superficial and truly deep activity resulted in CS suppression by the regression itself. In any case, the sex block proved that the regression-based cleaning procedure was quite effective, which reinforces the cerebral origin of responses to violence. In fact, we suggest using emotional stimuli with an identifiable effect on surface activity to check the reliability of signal denoising methods. Moreover, we firmly support the need for controlling surface interference, especially when using emotional stimulation.

4.2. Shared responses to violence pictures

We found significant ISCs associated with violence pictures, but only in the slowest component C9 (0 – 0.019 Hz) of CS. This finding is consistent with the fMRI study by (Kauppi et al., 2010), in which they found higher ISCs at similar low-frequencies (0 – 0.02 Hz) in prefrontal areas during emotional movie viewing. It has been suggested that higher order brain areas need to elaborate emotions for a long enough time to allow capturing coherent responses (Kauppi et al., 2010; Nastase et al., 2019).

A relevant finding was the observation of a reverse U-shaped HbO response coupled with opposite changes in HbR (Fig. 5). Previous fNIRS studies using IAPS found mixed results on HbO changes in PFC, for example: decreased dorsolateral HbO with positive stimuli and increased ventrolateral HbO with negative ones (Hoshi et al., 2011); increased dorsolateral HbO with positive and increased medial HbO with negative (Yukselen et al., 2023); increased HbO with negative pictures compared to neutral ones (Glotzbach et al., 2011): decreased HbO for negatives (Huang et al., 2017); no differences (Herrmann et al., 2003). Since other methods of emotion induction also yielded inconsistent results, differences in experimental design may be a likely cause (Bendall et al., 2016). Among other reasons, discrepancies could be due to (i) sample inhomogeneity, (ii) inappropriate response models, (iii) inconsistent removal of low frequencies, and (iv) interference from extracerebral activity. Note that our results would not be influenced by these four biasing factors.

At this point, it should be noted that the parcellation of the PFC varies among studies and that the RMPFC (our target) has often been included within the VMPFC (Dixon et al., 2017). The inverse oxygenation pattern would agree better with previous fMRI studies using IAPS, in which participants were asked to judge pictures as positive or negative by pressing response buttons (similarly to us). Significant negative BOLD responses (NBRs) were found in the VMPFC associated with negative valence (Grimm et al., 2009), or concurrent signal decreases in medial PFC (MPFC) with increases in lateral PFC (LPFC) counterparts (Northoff et al., 2004), and also decreases in orbital and dorsal parts of medial PFC with negative valence (Heinzel et al., 2005).

Given that facial expressions were clearly visible (mostly fearful and angry faces), our results would also agree with fMRI studies that found greater VMPFC deactivation for faces showing negative expressions (Sreenivas et al., 2012) and specifically for sad and fearful ones (Jamieson et al., 2021).

The observed response could be understood from the reciprocal attenuation effect suggested in the study by (Northoff et al., 2004), in which they found BOLD signal decreases in MPFC along with increases in LPFC during both emotional and non-emotional judgment of negative IAPS scenes. A valence-dependent coupling between the MPFC, LPFC and amygdala during emotional face processing has been highlighted (Willinger et al., 2019), in particular the stronger negative connectivity VMPFC to amygdala, along with positive connectivity amygdala to LPFC, induced by fearful expressions (Jamieson et al., 2021). Ample evidence points to the mediating role of VMPFC in inhibiting negative emotions through interaction with the amygdala and other brain structures (Hiser & Koenigs, 2018). However, given that both increased and decreased VMPFC activity in response to negative emotions has been described in either passive exposure or active regulation fMRI studies (Yang et al., 2020), it remains unclear when particular VMPFC subregions are activated/deactivated.

The response also may relate to the role of the VMPFC within the default mode network (DMN) (Raichle et al., 2001), as a result of the complex activations/deactivations driven by the interaction between DMN, such as those involving emotion regulation and judgments (Menon, 2023). Though VMPFC and DMN has been widely highlighted in studies of emotion, their precise role and interaction with other large-scale brain networks remains unclear (Satpute & Lindquist, 2019).

We acknowledge that these arguments are somewhat speculative because our NIRS device only probes a rostromedial portion of the PFC, without reaching more dorsal, lateral or deep parts. Furthermore, participants were not instructed on how to manage affective states and, with researchers being present, a spontaneous emotional regulation effect cannot be ignored (Morawetz et al., 2017). Moreover, given that both positive and negative correlations have been found between fNIRS and BOLD signals in, among others, prefrontal regions, it remains unclear how these signals are related (Wijeakumar et al., 2017), and also

whether BOLD activity would either reflect activations, inhibitions, or both (Lindquist et al., 2016). Therefore, although tempting, associating the observed response with a decrease in cortical activity is rather questionable. The slow U-shaped fluctuation of HbO (and the opposite change of HbR) could even reflect a progressive background consumption of oxygen due to increased activity that is also slowly compensated by blood flow. In any case, in view of the consistency of the fNIRS responses, intra-record judgments and SAM ratings, we are reasonably sure that the observed pattern somehow reflects a piece of the processing of violence content.

4.3. Shared responses to sexual pictures

Nearly all channels showed consistent responses at the lowest frequency for surface HbO within the sexual and the following neutral block. The latter was probably due to a "persistence effect" (Doi et al., 2013; León-Carrión et al., 2007), which underlines the importance of interleaving neutral stimulus time.

The sharp and sustained increase in HbO (Fig. 5), along with coupled HbR fluctuations, would reflect blood flow/volume changes in forehead vessels driven by systemic and/or local autonomic responses (Minati et al., 2009; Scholkmann et al., 2014). Photoplethysmographic and thermal imaging studies have often related forehead vasomotor reactivity with emotional states (Ioannou et al., 2014), such as embarrassment and shyness in women (Drummond, 1999; Ioannou et al., 2017). We are currently unable to properly discuss the triggering mechanisms, but believe they are related to blushing responses (Crozier and De Jong, 2012; Drummond and Su, 2012), sexual arousal (DePesa & Cassisi, 2017), or mixed effects. In contrast to later SAM ratings, inconsistent intra-record judgments may support a social shame reaction of certain participants due to the presence of others. Interpretations aside, the observed pattern is quite robust and clearly related to a distinctive extracerebral response to sexual content. Note that without short-channels it could be misinterpreted as of cerebral origin. We found no coherent responses in CS, which is consistent with fMRI studies reporting lower or no significant BOLD responses to sexual images in the medial PFC of heterosexual women (Jacob et al., 2011; Putkinen et al., 2023). However, as previously mentioned, an over regression effect that suppressed a highly correlated deep signal cannot be fully ruled out.

5. Limitations

The modest size and gender specificity of the sample limit the generalizability of our results. However, the enrollment of only women within a narrow age range may rather be a strength of the study. The low spatial resolution of fNIRS and individual anatomical differences in optode placement may have blurred the responses, degrading the ISC analysis. For multiresolution analysis we used wavelet filters not determined on a physiological basis, so a tailored filter-bank could improve the results. We used a unique IAPS sequence without inverting the order of presentation of the sexual and violence blocks. Future research is warranted to overcome these limitations, including larger samples and replicating this work also with men and different emotional stimuli.

6. Conclusion

This study is the first to combine sequential blocks of affective pictures with frequency-based ISC analysis to capture shared fNIRS responses to emotional content across participants. We extended conventional ISC paradigms to a block design in which pictures were presented at exactly the same time for all participants while multi-distance fNIRS signals were recorded on the forehead. Wavelet decomposition and permutation methods were applied to locate frequency-bands showing significant ISC. As a proof-of-concept, we found that the responses of young healthy women to sexual and violent content are differentiable and mainly localized in slow fluctuations of extracerebral and cerebral origin, respectively. As expected, we confirm the marked influence of surface hemodynamics on the deep fNIRS signals but, on the other hand, that it also contains valuable information. Although further work is needed, the proposed approach holds promise as a feasible tool for exploring functional biomarkers of healthy and altered emotional processing.

CRediT authorship contribution statement

S. Molina-Rodriguez: Conceptualization, Formal analysis, Investigation, Methodology, Writing – original draft. **C. Tabernero:** Conceptualization, Writing – review & editing. **J. Ibañez-Ballesteros:** Conceptualization, Formal analysis, Data curation, Methodology, Software, Supervision, Writing – original draft, Writing – review & editing.

Declaration of Generative AI and AI-assisted technologies in the writing process

The author(s) did not use generative AI technologies for preparation of this work

Funding

This work was conducted in absence of any funding.

Declaration of competing interest

JIB reports that he is inventor of patents licensed to Newmanbrain, SL and co-founder and scientific advisor of Newmanbrain S.L., the company responsible of manufacturing the NIRS device used in this research.

Declaration of Competing Interest

The authors declare the following financial interests/personal relationships which may be considered as potential competing interests: Joaquin Ibanez-Ballesteros reports equipment, drugs, or supplies was provided by Newmanbrain, SL. Joaquin Ibanez-Ballesteros reports a relationship with Newmanbrain, SL that includes: equity or stocks. Joaquin Ibanez-Ballesteros has patent licensed to Newmanbrain, SL. If there are other authors, they declare that they have no known competing financial interests or personal relationships that could have appeared to influence the work reported in this paper.

Acknowledgments

We sincerely thank professor Carlos Belmonte for his support and critical reading of the manuscript. We acknowledge the technical assistance of Mr. Miguel Ibañez and Mr. Alejandro Mendez.

Data Availability

Data will be made available on request.

References

Adolphs, R., Nummenmaa, L., Todorov, A., & Haxby, J. V. (2016). Data-driven approaches in the investigation of social perception. *Philosophical Transactions of the Royal Society B: Biological Sciences, 371*(1693). https://doi.org/10.1098/rstb.2015.0367

Arne, E. (2013). How and when the fMRI BOLD signal relates to underlying neural activity: The danger in dissociation. *Brain Res Rev, 62*(2), 233–244. https://doi.org/10.1016/j.brainresrev.2009.12.004.How

Bendall, R. C. A., Eachus, P., & Thompson, C. (2016). A brief review of research using near-infrared spectroscopy to measure activation of the prefrontal cortex during emotional processing: The importance of experimental design. *Frontiers in Human Neuroscience, 10*(OCT2016), 1–7. https://doi.org/10.3389/fnhum.2016.00529

Benjamini, Y., & Hochberg, Y. (1995). Controlling the false discovery rate - a practical and powerful approach to multiple testing. *J Royal Statist Soc, Series B, 57*, 289–300. https://doi.org/10.2307/2346101

Bermond, B., Bierman, D. J., Cladder, M. A., Moormann, P. P., & Vorst, H. C. M. (2010). The cognitive and affective alexithymia dimensions in the regulation of sympathetic responses. *International Journal of Psychophysiology, 75*(3), 227–233. https://doi.org/10.1016/j.ijpsycho.2009.11.004

Bolt, T., Nomi, J. S., Vij, S. G., Chang, C., & Uddin, L. Q. (2018). Inter-subject phase synchronization for exploratory analysis of task-fMRI. *NeuroImage, 176*(October 2017), 477–488. https://doi.org/10.1016/j.neuroimage.2018.04.015

Bradley, M., & Lang, P. J. (1994). Measuring emotion: the self-assessment manikin and the semantic differential. *Journal of Behavior Therapy and Experimental Psychiatry, 25*(1), 49–59.

Bradley, M. M., & Lang, P. J. (2007). The International Affective Picture System (IAPS) in the study of emotion and attention. In J. A. Coan, & J. J. B. Allen (Eds.), *Series in affective science.Handbook of emotion elicitation and assessment* (pp. 29–46). Oxford University Press.

Brigadoi, S., & Cooper, R. J. (2015). How short is short? optimum source–detector distance for short-separation channels in functional near-infrared spectroscopy. *Neurophotonics, 2*(2), Article 025005. https://doi.org/10.1117/1.nph.2.2.025005

Chen, G., Shin, Y.-W., Taylor, P. A., Glen, D. R., Reynolds, R. C., Israel, R. B., & Cox, R. W. (2016). Untangling the relatedness among correlations, part I: Nonparametric approaches to inter-subject correlation analysis at the group level. *NeuroImage, 142*(February 2018), 248–259. https://doi.org/10.1016/j.neuroimage.2016.05.023

Cohen, A., Daubechies, I., & Vial, P. (1993). Wavelets on the interval and fast wavelet transforms. *Applied and Computational Harmonic Analysis, 1*(1), 54–81. https://doi.org/10.1006/acha.1993.1005

Crozier, W., & De Jong, P. (2012). *The Psychological Significance of the Blush*. Cambridge University Press.

Cui, X., Bray, S., Bryant, D. M., Glover, G. H., & Reiss, A. L. (2011). A quantitative comparison of NIRS and fMRI across multiple cognitive tasks. *NeuroImage, 54*(4), 2808–2821. https://doi.org/10.1016/j.neuroimage.2010.10.069

Cyders, M. A., Dzemidzic, M., Eiler, W. J., & Kareken, D. A. (2016). An fMRI study of responses to sexual stimuli as a function of gender and sensation seeking: a preliminary analysis. *The Journal of Sex Research, 53*(8), 1020–1026. https://doi.org/10.1080/00224499.2015.1112340

Da Silva Ferreira Barreto, C., Zimeo Morais, G. A., Vanzella, P., & Sato, J. R. (2020). Combining the intersubject correlation analysis and the multivariate distance matrix regression to evaluate associations between fNIRS signals and behavioral data from ecological experiments. *Experimental Brain Research, 238*(10), 2399–2408. https://doi.org/10.1007/s00221-020-05895-8

Daubechies, I. (1992). *Ten Lectures On Wavelets*. Society for Industrial and Applied Mathematics.

Delpy, D. T., Cope, M., Van Der Zee, P., Arridge, S., Wray, S., & Wyatt, J. (1988). Estimation of optical pathlength through tissue from direct time of flight measurement. *Physics in Medicine and Biology, 33*(12), 1433–1442. https://doi.org/10.1088/0031-9155/33/12/008

DePesa, N. S., & Cassisi, J. E. (2017). Affective and autonomic responses to erotic images: evidence of disgust-based mechanisms in female sexual interest/arousal disorder. *Journal of Sex Research, 54*(7), 877–886. https://doi.org/10.1080/00224499.2016.1252307

Dixon, M. L., Thiruchselvam, R., & Christoff, K. (2017). Emotion and the prefrontal cortex: an integrative review. *Psychological Bulletin, 143*(10), 1033. https://doi.org/10.1037/bul0000096

Doi, H., Nishitani, S., & Shinohara, K. (2013). NIRS as a tool for assaying emotional function in the prefrontal cortex. *Frontiers in Human Neuroscience, NOV*. https://doi.org/10.3389/fnhum.2013.00770

Drummond, P. D. (1999). Facial flushing during provocation in women. *Psychophysiology, 36*(3), 325–332. https://doi.org/10.1017/S0048577299980344

Drummond, P. D., & Su, D. (2012). The relationship between blushing propensity, social anxiety and facial blood flow during embarrassment. *Cognition Emotion, 26*(3), 561–567. https://doi.org/10.1080/02699931.2011.595775

Erdoğan, S. B., Yücel, M. A., & Akın, A. (2014). Analysis of task-evoked systemic interference in fNIRS measurements: Insights from fMRI. *NeuroImage, 87*, 490–504. https://doi.org/10.1016/j.neuroimage.2013.10.024

Faraone, S. V., Banaschewski, T., Coghill, D., Zheng, Y., Biederman, J., Bellgrove, M. A., Newcorn, J. H., Gignac, M., Al Saud, N. M., Manor, I., Rohde, L. A., Yang, L., Cortese, S., Almagor, D., Stein, M. A., Albatti, T. H., Aljoudi, H. F., Alqahtani, M. M. J., Asherson, P., & Wang, Y. (2021). The World Federation of ADHD International Consensus Statement: 208 Evidence-based conclusions about the disorder. *Neuroscience and Biobehavioral Reviews, 128*(June 2020), 789–818. https://doi.org/10.1016/j.neubiorev.2021.01.022

Finn, E. S., Scheinost, D., Finn, D. M., Shen, X., Papademetris, X., & Constable, R. T. (2017). Can brain state be manipulated to emphasize individual differences in functional connectivity? *NeuroImage, 160*, 140–151. https://doi.org/10.1016/j.neuroimage.2017.03.064

Gagnon, L., Cooper, R. J., Yücel, M. A., Perdue, K. L., Greve, D. N., & Boas, D. A. (2012). Short separation channel location impacts the performance of short channel regression in NIRS. *NeuroImage, 59*(3), 2518–2528. https://doi.org/10.1016/j.neuroimage.2011.08.095

Gagnon, L., Perdue, K., Greve, D. N., Goldenholz, D., Kaskhedikar, G., & Boas, D. A. (2011). Improved recovery of the hemodynamic response in diffuse optical imaging using short optode separations and state-space modeling. *NeuroImage, 56*(3), 1362–1371. https://doi.org/10.1016/j.neuroimage.2011.03.001

Gagnon, L., Yücel, M. A., Boas, D. A., & Cooper, R. J. (2014). Further improvement in reducing superficial contamination in NIRS using double short separation measurements. *NeuroImage, 85*, 127–135. https://doi.org/10.1016/j.neuroimage.2013.01.073

Glotzbach, E., Mühlberger, A., Gschwendtner, K., Fallgatter, A. J., Pauli, P., & Herrmann, M. J. (2011). Prefrontal brain activation during emotional processing: a functional near infrared spectroscopy study (fNIRS). *The Open Neuroimaging Journal, 5*, 33–39. https://doi.org/10.2174/1874440001105010033

Grimm, S., Boesiger, P., Beck, J., Schuepbach, D., Bermpohl, F., Walter, M., Ernst, J., Hell, D., Boeker, H., & Northoff, G. (2009). Altered negative BOLD responses in the default-mode network during emotion processing in depressed subjects. *Neuropsychopharmacology, 34*(4), 932–943. https://doi.org/10.1038/npp.2008.81

Groen, Y., Wijers, A. A., Tucha, O., & Althaus, M. (2013). Neuropsychologia are there sex differences in ERPs related to processing empathy-evoking pictures ? *Neuropsychologia, 51*(1), 142–155. https://doi.org/10.1016/j.neuropsychologia.2012.11.012

Haeussinger, F. B., Heinzel, S., Hahn, T., Schecklmann, M., Ehlis, A. C., & Fallgatter, A. J. (2011). Simulation of near-infrared light absorption considering individual head and prefrontal cortex anatomy: Implications for optical neuroimaging. *PLoS ONE, 6*(10). https://doi.org/10.1371/journal.pone.0026377

Hasson, U., Nir, Y., Levy, I., Fuhrmann, G., & Malach, R. (2004). Intersubject synchronization of cortical activity during natural vision. *Science, 303*(5664), 1634–1640. https://doi.org/10.1126/science.1089506

Hasson, U., Yang, E., Vallines, I., Heeger, D. J., & Rubin, N. (2008). A hierarchy of temporal receptive windows in human cortex. *Journal of Neuroscience, 28*(10), 2539–2550. https://doi.org/10.1523/JNEUROSCI.5487-07.2008

Heinzel, A., Bermpohl, F., Niese, R., Pfennig, A., Pascual-Leone, A., Schlaug, G., & Northoff, G. (2005). How do we modulate our emotions? parametric fMRI reveals cortical midline structures as regions specifically involved in the processing of emotional valences. *Cognitive Brain Research, 25*(1), 348–358. https://doi.org/10.1016/j.cogbrainres.2005.06.009

Hejnar, M. P., Kiehl, K. A., & Calhoun, V. D. (2007). Interparticipant correlations: a model free FMRI analysis technique. *Human Brain Mapping, 28*(9), 860–867. https://doi.org/10.1002/hbm.20321

Herrmann, M. J., Ehlis, A. C., & Fallgatter, A. J. (2003). Prefrontal activation through task requirements of emotional induction measured with NIRS. *Biological Psychology, 64*(3), 255–263. https://doi.org/10.1016/S0301-0511(03)00095-4

Hiser, J., & Koenigs, M. (2018). The multifaceted role of the ventromedial prefrontal cortex in emotion, decision making, social cognition, and psychopathology. *Biological Psychiatry, 83*(8), 638–647. https://doi.org/10.1016/j.biopsych.2017.10.030

Hoshi, Y., Huang, J., Kohri, S., Iguchi, Y., Naya, M., Okamoto, T., & Ono, S. (2011). Recognition of human emotions from cerebral blood flow changes in the frontal region: a study with event-related near-infrared spectroscopy. *Journal of Neuroimaging, 21*(2), 94–101. https://doi.org/10.1111/j.1552-6569.2009.00454.x

Huang, Y., Mao, M., Zhang, Z., Zhou, H., Zhao, Y., Duan, L., Kreplin, U., Xiao, X., & Zhu, C. (2017). Test–retest reliability of the prefrontal response to affective pictures based on functional near-infrared spectroscopy. *Journal of Biomedical Optics, 22*(1), Article 016011. https://doi.org/10.1117/1.jbo.22.1.016011

Huppert, T. J., Diamond, S. G., Franceschini, M. A., & Boas, D. A. (2009). HomER: A review of time-series analysis methods for near-infrared spectroscopy of the brain. *Applied Optics, 48*(10), 0–33. https://doi.org/10.1364/AO.48.00D280

Ioannou, S., Gallese, V., & Merla, A. (2014). Thermal infrared imaging in psychophysiology: potentialities and limits. *Psychophysiology, 51*(10), 951–963. https://doi.org/10.1111/psyp.12243

Ioannou, S., Morris, P. H., Baker, M., Reddy, V., & Gallese, V. (2017). Seeing a blush on the visible and invisible spectrum: a functional thermal infrared imaging study. *Frontiers in Human Neuroscience, 11*(ember). https://doi.org/10.3389/fnhum.2017.00525

Jääskeläinen, I. P., Koskentalo, K., Balk, M. H., Autti, T., Kauramäki, J., Pomren, C., & Sams, M. (2008). Inter-subject synchronization of prefrontal cortex hemodynamic activity during natural viewing. *The Open Neuroimaging Journal, 2*(1), 14–19. https://doi.org/10.2174/1874440000802010014

Jacob, G. A., Arntz, A., Domes, G., Reiss, N., & Siep, N. (2011). Positive erotic picture stimuli for emotion research in heterosexual females. *Psychiatry Research, 190*(2–3), 348–351. https://doi.org/10.1016/j.psychres.2011.05.044

Jamieson, A. J., Davey, C. G., & Harrison, B. J. (2021). Differential modulation of effective connectivity in the brain's extended face processing system by fearful and sad facial expressions. *Eneuro, 8*(2), Article ENEURO.0380-20.2021. https://doi.org/10.1523/ENEURO.0380-20.2021

Kajimura, S., Margulies, D., & Smallwood, J. (2023). Frequency-specific brain network architecture in resting-state fMRI. *Scientific Reports, 13*(1), 1–9. https://doi.org/10.1038/s41598-023-29321-5

Kauppi, J. P., Jääskeläinen, I. P., Sams, M., & Tohka, J. (2010). Inter-subject correlation of brain hemodynamic responses during watching a movie: Localization in space and frequency. *Frontiers in Neuroinformatics, 4*(MAR), 1–10. https://doi.org/10.3389/fninf.2010.00005

Kauppi, J. P., Pajula, J., & Tohka, J. (2014). A versatile software package for inter-subject correlation based analyses of fMRI. *Frontiers in Neuroinformatics, 8*(JAN), 1–13. https://doi.org/10.3389/fninf.2014.00002

Kirilina, E., Jelzow, A., Heine, A., Niessing, M., Wabnitz, H., Brühl, R., Ittermann, B., Jacobs, A. M., & Tachtsidis, I. (2012). The physiological origin of task-evoked systemic artefacts in functional near infrared spectroscopy. *NeuroImage, 61*(1), 70–81. https://doi.org/10.1016/j.neuroimage.2012.02.074

Kocsis, L., Herman, P., & Eke, A. (2006). The modified Beer-Lambert law revisited. *Physics in Medicine and Biology, 51*(5). https://doi.org/10.1088/0031-9155/51/5/N02

Krishnamoorthy, K., & Xia, Y. (2007). Inferences on correlation coefficients: One-sample, independent and correlated cases. *Journal of Statistical Planning and Inference, 137*(7), 2362–2379. https://doi.org/10.1016/j.jspi.2006.08.002

Kurihara, K., Kawaguchi, H., Obata, T., Ito, H., Sakatani, K., & Okada, E. (2012). The influence of frontal sinus in brain activation measurements by near-infrared spectroscopy analyzed by realistic head models. *Biomedical Optics Express, 3*(9), 2121. https://doi.org/10.1364/boe.3.002121

León-Carrión, J., Martín-Rodríguez, J. F., Damas-López, J., Pourrezai, K., Izzetoglu, K., Barroso y Martin, J. M., & Domínguez-Morales, M. R. (2007). A lasting post-stimulus activation on dorsolateral prefrontal cortex is produced when processing valence and arousal in visual affective stimuli. *Neuroscience Letters, 422*(3), 147–152. https://doi.org/10.1016/j.neulet.2007.04.087

Lerner, Y., Honey, C. J., Silbert, L. J., & Hasson, U. (2011). Topographic mapping of a hierarchy of temporal receptive windows using a narrated story. *Journal of Neuroscience, 31*(8), 2906–2915. https://doi.org/10.1523/JNEUROSCI.3684-10.2011

Li, G., Zhang, S., Le, T. M., Tang, X., & Li, C. S. R. (2020). Neural responses to negative facial emotions: Sex differences in the correlates of individual anger and fear traits. *NeuroImage, 221*(June), Article 117171. https://doi.org/10.1016/j.neuroimage.2020.117171

Lindquist, K. A., Satpute, A. B., Wager, T. D., Weber, J., & Barrett, L. F. (2016). The brain basis of positive and negative affect: evidence from a meta-analysis of the human neuroimaging literature. *Cerebral Cortex, 26*(5), 1910–1922. https://doi.org/10.1093/cercor/bhv001

Mallat, S. (2008). *A wavelet tour of signal processing: the sparse way* (3rd ed.).). Academic Press.

Maruoka, K., Ooi, T., & Kano, T. (2007). Design of chiral organocatalysts for practical asymmetric synthesis of amino acid derivatives. *Chem Commun*, (15), 1487–1495. https://doi.org/10.1039/B613049F

Menon, V. (2023). 20 years of the default mode network: a review and synthesis. *Neuron, 111*(16), 2469–2487. https://doi.org/10.1016/j.neuron.2023.04.023

Minati, L., Jones, C. L., Gray, M. A., Medford, N., Harrison, N. A., & Critchley, H. D. (2009). Emotional modulation of visual cortex activity: a functional near-infrared spectroscopy study. *NeuroReport, 20*(15), 1344–1350. https://doi.org/10.1097/WNR.0b013e328330c751

Molina-Rodríguez, S., Mirete-Fructuoso, M., Martínez, L. M., & Ibañez-Ballesteros, J. (2022). Frequency-domain analysis of fNIRS fluctuations induced by rhythmic mental arithmetic. *Psychophysiology, 59*(10). https://doi.org/10.1111/psyp.14063

Moltó, J., Segarra, P., López, R., Esteller, À., Fonfría, A., & Pastor, M. C. (2013). Adaptación española del – international affective picture system (IAPS). Tercera parte. *Anales Délelőtt Psicologia, 29*(3), 965–984.

Morawetz, C., Bode, S., Derntl, B., & Heekeren, H. R. (2017). The effect of strategies, goals and stimulus material on the neural mechanisms of emotion regulation: a meta-analysis of fMRI studies. *Neuroscience and Biobehavioral Reviews, 72*, 111–128. https://doi.org/10.1016/j.neubiorev.2016.11.014

Nam, C. S., Choo, S., Huang, J., & Park, J. (2020). Brain-to-brain neural synchrony during social interactions: a systematic review on hyperscanning studies. *Applied Sciences (Switzerland), 10*(19), 1–23. https://doi.org/10.3390/APP10196669

Nastase, S. A., Gazzola, V., Hasson, U., & Keysers, C. (2019). Measuring shared responses across subjects using intersubject correlation. *Social Cognitive and Affective Neuroscience, 14*(6), 669–687. https://doi.org/10.1093/scan/nsz037

Nichols, T. E., & Holmes, A. P. (2002). Nonparametric permutation tests for functional neuroimaging: a primer with examples. *Human Brain Mapping, 15*(1), 1–25. https://doi.org/10.1002/hbm.1058

Northoff, G., Heinzel, A., Bermpohl, F., Niese, R., Pfennig, A., Pascual-Leone, A., & Schlaug, G. (2004). Reciprocal modulation and attenuation in the prefrontal cortex: an fMRI study on emotional-cognitive interaction. *Human Brain Mapping, 21*(3), 202–212. https://doi.org/10.1002/hbm.20002

Nummenmaa, L., Glerean, E., Viinikainen, L. P., Jaaskelainen, I. P., Hari, R., & Sams, M. (2012). Emotions promote social interaction by synchronizing brain activity across individuals. *Proceedings of the National Academy of Sciences, 109*(24), 9599–9604. https://doi.org/10.1073/pnas.1206095109

Orihuela-Espina, F., Leff, D. R., James, D. R. C., Darzi, A. W., & Yang, G. Z. (2010). Quality control and assurance in functional near infrared spectroscopy (fNIRS) experimentation. *Physics in Medicine and Biology, 55*(13), 3701–3724. https://doi.org/10.1088/0031-9155/55/13/009

Pajula, J., Kauppi, J. P., & Tohka, J. (2012). Inter-subject correlation in fMRI: Method validation against stimulus-model based analysis. *PLoS ONE, 8*, *7*. https://doi.org/10.1371/journal.pone.0041196

Pajula, J., & Tohka, J. (2016). How many is enough? effect of sample size in inter-subject correlation analysis of fMRI. *Computational Intelligence and Neuroscience, 2016*. https://doi.org/10.1155/2016/2094601

Percival, D. B., & Walden, A. T. (2000). *Wavelet Methods for Time SeriesAnalysis*. Cambridge University Press. https://doi.org/10.1017/CBO9780511841040

Pfeifer, M. D., Scholkmann, F., & Labruyère, R. (2018). Signal processing in functional near-infrared spectroscopy (fNIRS): methodological differences lead to different statistical results. *Frontiers in Human Neuroscience, 11*. https://doi.org/10.3389/fnhum.2017.00641

Pinti, P., Tachtsidis, I., Hamilton, A., Hirsch, J., Aichelburg, C., Gilbert, S., & Burgess, P. W. (2018). The present and future use of functional near-infrared spectroscopy (fNIRS) for cognitive neuroscience. *Annals of the New York Academy of Sciences*, 1–25. https://doi.org/10.1111/nyas.13948

Putkinen, V., Nazari-Farsani, S., Karjalainen, T., Santavirta, S., Hudson, M., Seppälä, K., Sun, L., Karlsson, H. K., Hirvonen, J., & Nummenmaa, L. (2023). Pattern recognition reveals sex-dependent neural substrates of sexual perception. *Human Brain Mapping, 44*(6), 2543–2556. https://doi.org/10.1002/hbm.26229

Raghunathan, T. E., Rosenthal, R., & Rubin, D. B. (1996). Comparing correlated but nonoverlapping correlations. *Psychological Methods, 1*(2), 178–183. https://doi.org/10.1037/1082-989X.1.2.178

Raichle, M. E., MacLeod, A. M., Snyder, A. Z., Powers, W. J., Gusnard, D. A., & Shulman, G. L. (2001). A default mode of brain function. *Proceedings of the National Academy of Sciences of the United States of America, 98*(2), 676–682. https://doi.org/10.1073/pnas.98.2.676

Rhif, M., Ben Abbes, A., Farah, I., Martínez, B., & Sang, Y. (2019). Wavelet transform application for/in non-stationary time-series analysis: a review. *Applied Sciences, 9*(7), 1345. https://doi.org/10.3390/app9071345

Ritz, T., Thöns, M., Fahrenkrug, S., & Dahme, B. (2005). Airways, respiration, and respiratory sinus arrhythmia during picture viewing. *Psychophysiology, 42*(5), 568–578. https://doi.org/10.1111/j.1469-8986.2005.00312.x

Rowland, S. C., Hartley, D. E. H., & Wiggins, I. M. (2018). Listening in naturalistic scenes: what can functional near-infrared spectroscopy and intersubject correlation analysis tell us about the underlying brain activity? *Trends in Hearing, 22*, 1–18. https://doi.org/10.1177/2331216518804116

Saager, R. B., & Berger, A. (2008). Measurement of layer-like hemodynamic trends in scalp and cortex: implications for physiological baseline suppression in functional near-infrared spectroscopy. *Journal of Biomedical Optics, 13*(3), Article 034017. https://doi.org/10.1117/1.2940587

Saager, R. B., & Berger, A. J. (2005). Direct characterization and removal of interfering absorption trends in two-layer turbid media. *Journal of the Optical Society of America A, 22*(9), 1874. https://doi.org/10.1364/josaa.22.001874

Saager, R. B., Telleri, N. L., & Berger, A. J. (2011). Two-detector Corrected Near Infrared Spectroscopy (C-NIRS) detects hemodynamic activation responses more robustly than single-detector NIRS. *NeuroImage, 55*(4), 1679–1685. https://doi.org/10.1016/j.neuroimage.2011.01.043

Saarimäki, H. (2021). Naturalistic stimuli in affective neuroimaging: a review. *Frontiers in Human Neuroscience, 15*(June). https://doi.org/10.3389/fnhum.2021.675068

Sato, H., Yahata, N., Funane, T., Takizawa, R., Katura, T., Atsumori, H., Nishimura, Y., Kinoshita, A., Kiguchi, M., Koizumi, H., Fukuda, M., & Kasai, K. (2013). A NIRS-fMRI investigation of prefrontal cortex activity during a working memory task. *NeuroImage, 83*, 158–173. https://doi.org/10.1016/j.neuroimage.2013.06.043

Satpute, A. B., & Lindquist, K. A. (2019). The default mode network's role in discrete emotion. *Trends in Cognitive Sciences, 23*(10), 851–864. https://doi.org/10.1016/j.tics.2019.07.003

Scarpa, F., Brigadoi, S., Cutini, S., Scatturin, P., Zorzi, M., Dell'Acqua, R., & Sparacino, G. (2013). A reference-channel based methodology to improve estimation of event-related hemodynamic response from fNIRS measurements. *NeuroImage, 72*, 106–119. https://doi.org/10.1016/j.neuroimage.2013.01.021

Scholkmann, F., Kleiser, S., Metz, A. J., Zimmermann, R., Mata Pavia, J., Wolf, U., & Wolf, M. (2014). A review on continuous wave functional near-infrared spectroscopy and imaging instrumentation and methodology. *NeuroImage, 85*, 6–27. https://doi.org/10.1016/j.neuroimage.2013.05.004

Scholkmann, F., & Wolf, M. (2013). General equation for the differential pathlength factor of the frontal human head depending on wavelength and age. *Journal of Biomedical Optics, 18*(10), Article 105004. https://doi.org/10.1117/1.jbo.18.10.105004

Silver, N. C., & Dunlap, W. P. (1987). Averaging correlation coefficients: should Fisher's z transformation be used? *Journal of Applied Psychology, 72*(1), 146–148. https://doi.org/10.1037/0021-9010.72.1.146

Simony, E., & Chang, C. (2020). Analysis of stimulus-induced brain dynamics during naturalistic paradigms. *NeuroImage, 216*(July 2019), Article 116461. https://doi.org/10.1016/j.neuroimage.2019.116461

Singh, A. K., & Dan, I. (2006). Exploring the false discovery rate in multichannel NIRS. *NeuroImage, 33*(2), 542–549. https://doi.org/10.1016/j.neuroimage.2006.06.047

Somech, N., Mizrahi, T., Caspi, Y., & Axelrod, V. (2022). Functional near-infrared spectroscopy imaging of the prefrontal cortex during a naturalistic comedy movie. *Frontiers in Neuroscience, 16*(September), 1–17. https://doi.org/10.3389/fnins.2022.913540

Sreenivas, S., Boehm, S. G., & Linden, D. E. J. (2012). Emotional faces and the default mode network. *Neuroscience Letters, 506*(2), 229–234. https://doi.org/10.1016/j.neulet.2011.11.012

Steinbrink, J., Villringer, A., Kempf, F., Haux, D., Boden, S., & Obrig, H. (2006). Illuminating the BOLD signal: combined fMRI-fNIRS studies. *Magnetic Resonance Imaging, 24*(4), 495–505. https://doi.org/10.1016/j.mri.2005.12.034

Stevens, J. S., & Hamann, S. (2012). Sex differences in brain activation to emotional stimuli: A meta-analysis of neuroimaging studies. *Neuropsychologia, 50*(7), 1578–1593. https://doi.org/10.1016/j.neuropsychologia.2012.03.011

Strangman, G. E., Li, Z., & Zhang, Q. (2013). Depth sensitivity and source-detector separations for near infrared spectroscopy based on the colin27 brain template. *PLoS ONE, 8*(8). https://doi.org/10.1371/journal.pone.0066319

Tachtsidis, I., & Scholkmann, F. (2016). False positives and false negatives in functional near-infrared spectroscopy: issues, challenges, and the way forward. *Neurophotonics, 3*(3), Article 031405. https://doi.org/10.1117/1.nph.3.3.031405

Takahashi, T., Takikawa, Y., Kawagoe, R., Shibuya, S., Iwano, T., & Kitazawa, S. (2011). Influence of skin blood flow on near-infrared spectroscopy signals measured on the forehead during a verbal fluency task. *NeuroImage, 57*(3), 991–1002. https://doi.org/10.1016/j.neuroimage.2011.05.012

Tuscan, L. A., Herbert, J. D., Forman, E. M., Juarascio, A. S., Izzetoglu, M., & Schultheis, M. (2013). Exploring frontal asymmetry using functional near-infrared spectroscopy: a preliminary study of the effects of social anxiety during interaction and performance tasks. *Brain Imaging and Behavior, 7*(2), 140–153. https://doi.org/10.1007/s11682-012-9206-z

Westgarth, M. M. P., Hogan, C. A., Neumann, D. L., & Shum, D. H. K. (2021). A systematic review of studies that used NIRS to measure neural activation during emotion processing in healthy individuals. *Social Cognitive and Affective Neuroscience, 16*(4), 345–369. https://doi.org/10.1093/scan/nsab017

Whittle, S., Yücel, M., Yap, M. B. H., & Allen, N. B. (2011). Sex differences in the neural correlates of emotion: Evidence from neuroimaging. *Biological Psychology, 87*(3), 319–333. https://doi.org/10.1016/j.biopsycho.2011.05.003

Wijeakumar, S., Huppert, T. J., Magnotta, V. A., Buss, A. T., & Spencer, J. P. (2017). Validating an image-based fNIRS approach with fMRI and a working memory task. *NeuroImage, 147*(December 2015), 204–218. https://doi.org/10.1016/j.neuroimage.2016.12.007

Willinger, D., Karipidis, I. I., Beltrani, S., Di Pietro, S. V., Sladky, R., Walitza, S., Stämpfli, P., & Brem, S. (2019). Valence-dependent coupling of prefrontal-amygdala effective connectivity during facial affect processing. *ENeuro, 6*(4), 1–12. https://doi.org/10.1523/ENEURO.0079-19.2019

Yamada, T., Umeyama, S., & Matsuda, K. (2012). Separation of fNIRS signals into functional and systemic components based on differences in hemodynamic modalities. *PLoS ONE, 7*(11). https://doi.org/10.1371/journal.pone.0050271

Yang, M., Tsai, S.-J., & Li, C.-S. R. (2020). Concurrent amygdalar and ventromedial prefrontal cortical responses during emotion processing: a meta-analysis of the effects of valence of emotion and passive exposure versus active regulation. *Brain Structure and Function, 225*(1), 345–363. https://doi.org/10.1007/s00429-019-02007-3

Yücel, M. A., Selb, J. J., Huppert, T. J., Franceschini, M. A., & Boas, D. A. (2017). Functional near infrared spectroscopy: enabling routine functional brain imaging. *Current Opinion in Biomedical Engineering, 4*, 78–86. https://doi.org/10.1016/j.cobme.2017.09.011

Yukselen, G., Ozturk, O. C., Canli, G. D., & Erdogan, S. B. (2023). Investigating the neural correlates of processing basic emotions: a functional near-infrared spectroscopy (fNIRS) Study. *BioRxiv*, 2008–2023. https://doi.org/10.1101/2023.08.08.551979

Zhang, Y., Tan, F., Xu, X., Duan, L., Liu, H., Tian, F., & Zhu, C.-Z. (2015). Multiregional functional near-infrared spectroscopy reveals globally symmetrical and frequency-specific patterns of superficial interference. *Biomedical Optics Express, 6*(8), 2786. https://doi.org/10.1364/boe.6.002786

Zimeo Morais, G. A., Scholkmann, F., Balardin, J. B., Furucho, R. A., de Paula, R. C. V., Biazoli, C. E., & Sato, J. R. (2017). Non-neuronal evoked and spontaneous hemodynamic changes in the anterior temporal region of the human head may lead to misinterpretations of functional near-infrared spectroscopy signals. *Neurophotonics, 5*(01), 1. https://doi.org/10.1117/1.nph.5.1.011002